Chemical Science

ROYAL SOCIETY OF CHEMISTRY

EDGE ARTICLE

View Article Online
View Journal | View Issue

Cite this: *Chem. Sci.*, 2025, **16**, 3275

All publication charges for this article have been paid for by the Royal Society of Chemistry

A comparative investigation on excimer fluorescence toward its bright future†

Shiyin Wang,[a] Haichao Liu, *[a] Shuaiqiang Zhao,[a] Qiaolin Wu,[b] Zhiqiang Yang,[a] Daojie Yang,[a] Yingbo Lv,[a] Qing Su,[b] Shi-Tong Zhang[a] and Bing Yang *[a]

Must excimers quench fluorescence? This study aims to clarify the misconception that excimers are defective species with weak fluorescence. For this purpose, we utilized a rigid xanthene template to connect anthracene units for constructing an inter-excimer and an intra-excimer. Their photophysical properties were systematically investigated in solution and crystal forms, representing dynamic and static environments, respectively. In solutions, the inter- and intra-excimers exhibited low fluorescence efficiencies due to the limited formation and ease of dissociation of the excimers. In crystals, the inter- and intra-excimers both demonstrated a significant increase in fluorescence efficiency, which was ascribed to the greatly suppressed non-radiation for the static excimer in a rigid environment. Furthermore, the efficiency of the inter-excimer was higher than that of the intra-excimer, which arose from the more stable excited state for more effective non-radiative suppression. Therefore, it was concluded that the probability and stability of excimer formation are the key factors for improving excimer fluorescence efficiency. Overall, their fluorescence efficiencies can be ranked as follows: dynamic inter-excimer < dynamic intra-excimer < static intra-excimer < static inter-excimer, which is subjected to environmental rigidity and excimer stability. This work will provide a comprehensive understanding of excimers and propose a novel design strategy to achieve high-efficiency fluorescent materials for innovative organic photo-functional applications.

Received 26th November 2024
Accepted 8th January 2025

DOI: 10.1039/d4sc08001g

rsc.li/chemical-science

Introduction

Achieving highly efficient organic fluorescent materials is a long-standing and enduring topic due to their significant value in many applications, such as optoelectronic devices, bio-imaging, and sensors.[1–10] Commonly used fluorescence molecules typically consist of planar rigid π-conjugation units, enabling high-efficiency fluorescence in a single-molecule state.[11–14] However, when presented as an ensemble in concentrated solutions or aggregates, these molecules are in turn prone to quenching their fluorescence due to the formation of detrimental species (*e.g.*, excimers) by intermolecular π–π stacking.[15–18] An 'excited dimer,' which is abbreviated as 'excimer,' is formed when an excited-state molecule associates with a ground-state molecule of the same type, as defined by Birks.[19–21] Dynamic excimers, according to Birks' definition, are frequently observed in fluid media (*e.g.*, liquid and gas).[22–24] Excimer formation in solution is a concentration-dependent and diffusion-controlled process, corresponding to the establishment of a dynamic balance between excimer fluorescence and monomer emission.[25–28] In fluid media, the environmental disturbance may decrease the rate of excimer formation and increase the chance of excimer dissociation, which promotes excimer deactivation along non-radiative pathways, especially in the case of forbidden radiative transition of excimers.[19,29–31] Consequently, excimers generally exhibit weak fluorescence for most π-conjugated fluorophores in fluid media, leading to the common sense tenet that excimers usually quench fluorescence as energy traps.[32–35]

To enhance excimer fluorescence efficiency, intramolecular dimers of some aromatic chromophores have been designed and synthesized using flexible alkyl chains[36–39] and rigid frames (*e.g.*, xanthene and triptycene scaffolds)[40–47] as bridging groups. Compared to noncovalent dimers that form intermolecular excimers (inter-excimers), these covalent dimers are usually expected to form intramolecular excimers (intra-excimers) with enhanced emission to a certain extent in solution. This enhancement is attributed to the faster formation and slower dissociation rates to afford the disturbance of the dynamic environment, together with the non-radiative suppression from the rigid bridge structures.[48–55] Some macrocyclic-based host–guest assemblies have been used to construct the noncovalent π–π dimer in an appropriately sized cavity, achieving enhanced excimer fluorescence in solution.[56–63]

[a]*State Key Laboratory of Supramolecular Structure and Materials, College of Chemistry, Jilin University, Changchun 130012, China. E-mail: hcliu@jlu.edu.cn; yangbing@jlu.edu.cn*

[b]*College of Chemistry, Jilin University, Changchun 130012, China*

† Electronic supplementary information (ESI) available: Synthetic details, theoretical calculations, and photophysical measurements. CCDC 2376432 and 2404819. For ESI and crystallographic data in CIF or other electronic format see DOI: https://doi.org/10.1039/d4sc08001g

However, macrocyclic-based host–guest assemblies have rarely been studied in solid states, due to their difficult crystallization caused by their large molecular weights. For further practical application, research has been focused on exploring static excimer formation in rigid media by designing and regulating π–π stacking between molecules.[64–77] Unlike a dynamic excimer, which is formed by initial excitation from a monomer, a static excimer can be generated by direct excitation from a pre-associated dimer in the ground state.[23,78] In a rigid environment, a static excimer can be effectively formed as long as there is sufficiently strong π–π stacking between the two pre-associated monomers.[45,79] Due to the non-radiative suppression in rigid media, some static excimers exhibit high-efficiency excimer fluorescence in crystals with discrete π–π stacking of intermolecular dimers, but in fact, most excimers do not significantly show this trend.[80–87]

For increased understanding of excimers and further exploration of their potential as emissive species, we strategically constructed two types of dimers (noncovalent and covalent), corresponding to inter-excimer and intra-excimer, using anthracene (AN) as a fluorophore (Scheme 1a). Their photophysical properties were systematically investigated in solutions (dynamic) and crystal (static) environments. In solutions, although the photoluminescence quantum yields (PLQYs) of both excimers are lower than that of monomer, the intra-excimer exhibits an increased PLQY compared to the inter-excimer due to the presence of a rigid frame template, which prompts formation and restricts dissociation of excimer. In crystals, the inter-excimer exhibits a higher PLQY compared to the intra-excimer, which can be ascribed to the greatly suppressed non-radiative transition of the inter-excimer. More importantly, inter-excimer is characterized by a more stable equilibrium geometry (anti-parallel face-to-face π–π stacking) in a discrete arrangement of AN dimer in the crystal, albeit being based on the forbidden emissive state of an excimer. As a whole, their PLQYs can be depicted in the order: dynamic inter-excimer < dynamic intra-excimer < static intra-excimer < static inter-excimer, which are subjected to environmental rigidity and excimer stability. These findings offer a new and valuable insight into the underlying mechanisms behind the high fluorescence efficiency induced by π–π stacked excimer in materials.

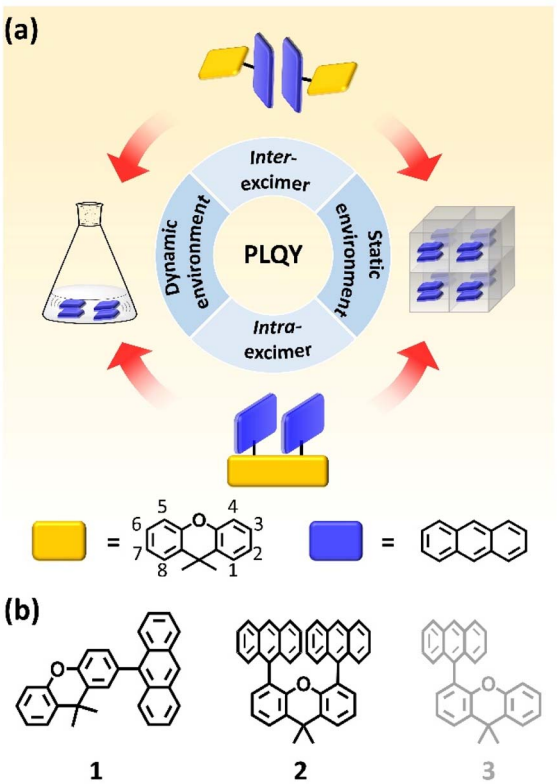

Scheme 1 (a) Diagram of the design strategy for inter-excimer and intra-excimer. (b) Molecular structures in this study, and **3** was used as a control molecule.

Results and discussion

Molecular design

Previously, our group reported a series of discretely dimeric π–π stacking motifs in crystals using an ingenious molecular design that incorporates a one-sided substituent into a planar π-fluorophore.[79–83,88–90] Due to the steric effect, the one-sided substituents force the two π-fluorophores to form anti-parallel π–π stacking so that the substituents located on both sides can act as spacers to isolate and protect the formed π–π dimer, thus preventing the infinite aggregation of π-fluorophores and constructing π–π dimers as discrete entities. Molecule **1** (Scheme 1b) was designed by incorporating 2-position xanthene as a sterically hindered unilateral substituent into AN, with the aim of achieving the inter-excimer in crystal based on the discrete AN dimer. Notably, the rational orientation of xanthene in molecule **1** is the key structural factor that facilitates the formation of anti-parallel π–π stacking between two AN units in the aggregate state. Molecule **2** (Scheme 1b) consists of two AN fluorophores and xanthene as a rigid linker template that enable construction of a covalent dimer of AN with well-defined π–π stacking for easy intra-excimer formation in fluid and rigid media.[41–46] This molecular design enhances excimer formation probability through pre-association facilitated by the rigid linker, mitigating non-radiative decay in dynamic excimers. Molecule **3** (Scheme 1b), analogous to molecule **2** but with a single AN unit, was designed for a precise comparison between excimer and monomer emissions. In molecule **3**, the orthogonal orientation of the 4-position xanthene relative to the AN plane creates a larger steric hindrance above the AN plane compared to the slant orientation of the 2-position xanthene. This larger steric hindrance in molecule **3** invalidates the formation of AN dimer in crystal.[80] These designed molecules are expected to facilitate the formation of an inter-excimer and intra-excimer in solutions and in crystals, respectively. Through systematic investigation of their photophysical properties, we aim to develop a comprehensive and in-depth understanding of excimer. The synthesis details are presented in the ESI.†

Excimers in a dynamic environment and their photophysical properties

Solvent-independent UV-visible (UV-vis) absorption and photoluminescence (PL) spectra were exhibited by **1** and **2** (Fig. S1†).

The UV-vis absorption and PL spectra of the two compounds in tetrahydrofuran (THF) solution are shown in Fig. 1a. Both compounds exhibit a similar absorption spectrum with the vibrational fine structure of an AN unit at 300–400 nm. Compared to **3**, **2** shows a slightly bathochromic absorption onset, which indicates the existence of ground-state interactions between two AN units (Fig. S2†). The PL spectrum of **1** exhibits the vibronic structure feature of AN fluorophore with $\lambda_{max} = 405$ nm, while the PL spectrum of **2** is strongly redshifted to 500 nm with broadened full width at half maximum (FWHM), which reveals a typical excimer emission character in the excited state. The PL spectrum of **2** in a concentrated solution is virtually identical to that in a dilute solution (Fig. 1b), excluding the possibility of inter-excimer formation.[46,48] The time-resolved PL spectra of **1** and **2** in diluted THF solutions show lifetimes of 5.28 ns and 18.69 ns, respectively, which correspond to monomer and excimer emission (Fig. 1c). Therefore, we can attribute the emission of **2** to intra-excimer fluorescence.

To observe the characteristics of the inter-excimer, the concentration-dependent PL spectra and aggregation-induced PL spectra were recorded (Fig. 1b and S3–S5†). With increasing concentration of **1** in THF solutions, a shoulder emission band was generated in the long-wavelength region when the concentration was 10^{-1} mol L^{-1} (Fig. 1b). The shoulder emission band peaked at 514 nm with an elongated lifetime (Fig. 1c), which was ascribed to the appearance of the inter-excimer of AN. The concentration-dependent experiment served to clearly distinguish the intra-excimer and inter-excimer of AN. Moreover, the crystal structure provides direct evidence for distinguishing between these two types of excimers (*vide infra*).

In addition to the different PL spectra and lifetimes between **1** and **2**, their PLQYs also differentiate by a large degree, at 47.04% for **1** and 12.86% for **2** in dilute THF solutions (Fig. 1d). Moreover, with increasing concentration of **1** in THF solutions, the PLQYs are obviously decreased, reaching 10.56% in a concentrated THF solution of 10^{-1} mol L^{-1}. In this case, the PLQY of pure inter-excimer was estimated to be 6.01% using peak fitting analysis of a PL spectrum (Fig. 1b and S6†). The low PLQYs of **2** in a dilute solution and **1** in a concentrated solution are in accordance with the viewpoint of excimer quenching fluorescence.[16–18] For an essential understanding of the excimer,

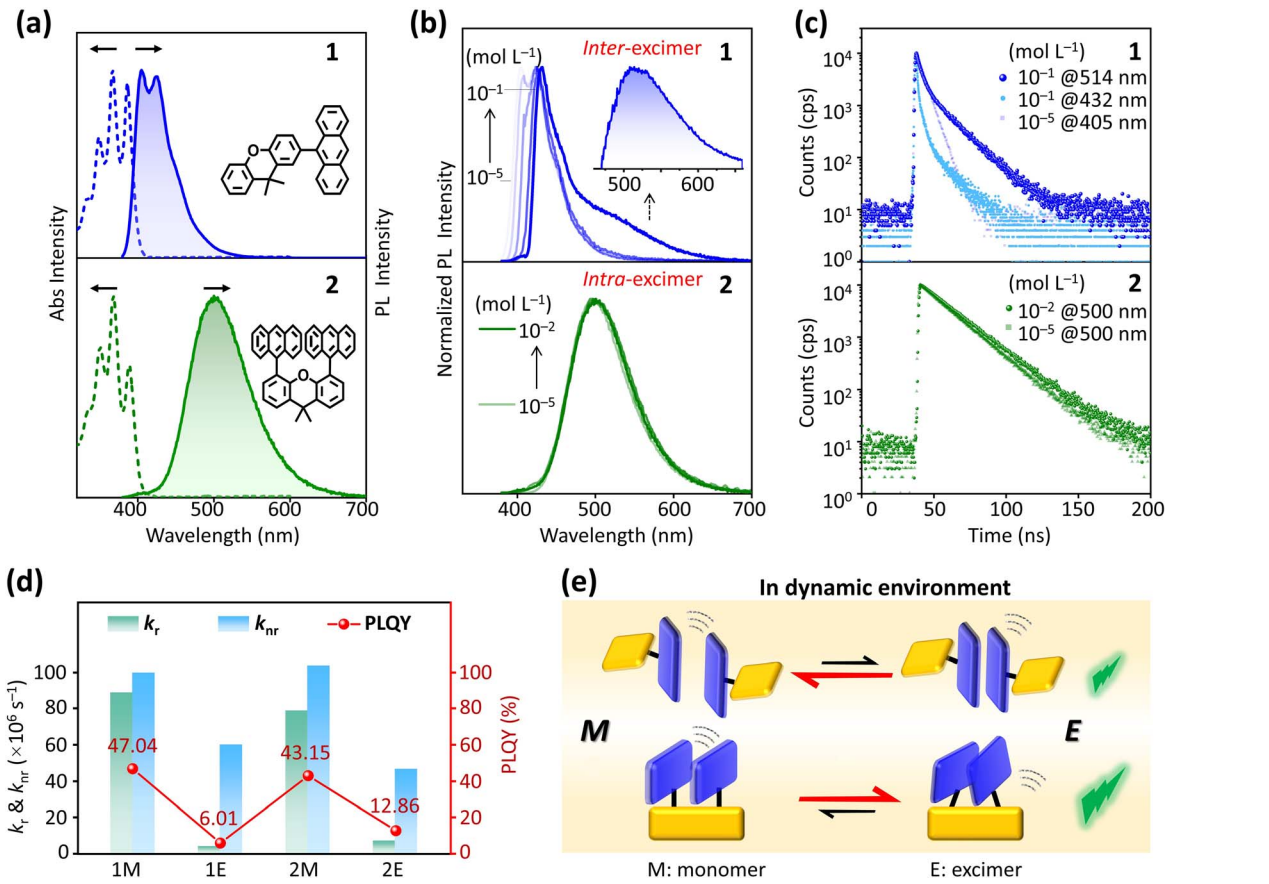

Fig. 1 (a) Absorption and PL spectra of **1** and **2** in diluted THF solutions, with the molecular structures of **1** and **2** inserted. (b) Concentration-dependent PL spectra of **1** and **2**. The inset shows the resolved excimer emission by deducting the spectrum of the low-concentration solution (10^{-5} mol L^{-1}) from that of the high-concentration solution (10^{-1} mol L^{-1}). (c) Time-resolved PL spectra of **1** and **2** in solutions of THF at different concentrations. (d) PLQYs, k_rs and k_{nr}s of monomers and excimers for **1** and **2**. The monomer of **2** is actually represented by **3** in diluted solution. (e) Schematic diagram of inter-excimer and intra-excimer in a dynamic environment. In a dynamic environment, intra-excimer forms more readily and is harder to dissociate than inter-excimer.

the radiative transition rate (k_r) and non-radiative transition rate (k_{nr}) were calculated according to the PLQY and lifetime values (Fig. 1d and Table S1†). Compared to the monomer (**1** and **3** in dilute solutions), the inter-excimer for **1** and the intra-excimer for **2** show a drastic decrease in k_r due to their forbidden nature of radiative transition (3.85×10^6 s^{-1} for the inter-excimer and 6.88×10^6 s^{-1} for the intra-excimer), which are in sharp contrast to 8.91×10^7 s^{-1} for monomer **1** and 7.90×10^7 s^{-1} for monomer **3**. Among these emissive species, the intra-excimer of **2** demonstrated the lowest k_{nr} value (4.66×10^7 s^{-1}), which can be attributed to the restrictive effect of the rigid xanthene scaffold. The restriction of the rigid frame contributes to the accelerated formation, slowed dissociation, and suppressed non-radiation of intra-excimer, resulting in an improved PLQY of intra-excimer compared to that of inter-excimer in solution (Fig. 1e).[30,31]

Overall, the dynamic inter-excimer and intra-excimer show weak fluorescence emission in solution, which is attributable to the inherently forbidden radiative transition nature of the excimer and the dominant non-radiative decay (including the non-radiative transition rate and excimer dissociation rate) caused by the dynamic environment. As an inspiration, the suppression of non-radiation should be the most effective method to improve the PLQY of excimer fluorescence, especially for reducing the dynamics of the environment.

Excimers in a static environment and their photophysical properties

Compared to the dynamic excimer in solution, the static excimer can be formed by the photoexcitation of the pre-associated dimer in a rigid environment. To achieve a rigid environment, single crystals of **1** and **2** were grown using the solvent diffusion method. Unfortunately, we were unable to collect crystals of molecule **3** (Fig. S7†). The details are provided in the ESI.† Consequently, bright green crystal **1** and blue-green crystal **2** were obtained and identified. Furthermore, PL spectra and time-resolved PL spectra were collected for the obtained crystals (Fig. 2a–c). Crystal **1** exhibits a strongly redshifted, structureless, and broadened PL spectrum peaking at 505 nm, along with an elongated lifetime of 152.7 ns. As we expected, these PL characteristics observed in crystal **1** are exactly in accordance with the inter-excimer emission of AN in a sandwich fashion (*vide infra*).[91] In contrast, the single crystal of **2** exhibits a redshifted, broadened, and structureless PL spectrum (λ_{max} = 478 nm) with a slightly long (40.36 ns) lifetime, which is consistent with the characteristics of an intra-excimer.[46] It is noteworthy that crystal **2** exhibits a shorter lifetime (Table S2†) and a blue-shifted PL spectrum compared to crystal **1**, although both are characterized by excimer emission.

A single-crystal X-ray diffraction (SCXRD) experiment was performed to investigate the molecular packing structures (Fig. 2d). Crystals of **1** are featured with a face-to-face antiparallel π–π stacking arrangement between AN units, in which each AN dimer is spatially separated from its neighbors by xanthene units, forming discrete π–π stacking dimers of AN, as we expected. The pairwise AN dimers in crystal **1** demonstrate a π–π distance ($d_{\pi-\pi}$) of 3.582 Å and an overlap ratio of 43.02%. The proper $d_{\pi-\pi}$ of AN dimer in crystal **1** is substantially responsible for inter-excimer formation, as evidenced by its unique PL properties. Moreover, these noncovalent dimers existing in crystal **1** can be regarded as a special case of self-limited assembly that prevents the growth of sizes beyond that of a dimer, as elucidated in the *Molecular design* section. These results further validate our design strategy of constructing discrete dimeric π–π stacking to minimize the interactions between dimers in crystal. As a comparison, in the **2** crystals, two AN units adopt a slightly misaligned face-to-face arrangement (dihedral angle = 10.20°). The average $d_{\pi-\pi}$ is 3.690 Å (Fig. S8 and Table S3†) between two AN planes in the vertical direction, with an overlap ratio of 65.56%. Thus, by designing the molecular structure and regulating the molecular packing, inter-excimer and intra-excimer emissions can be achieved based on noncovalent and covalent dimers of AN in crystals.

According to previous reports, a larger π–π overlap in a dimer usually leads to a more redshifted PL spectrum.[78,92] However, this rule does not apply to the **2** crystal. As a matter of fact, the initial π–π stacking (including the interplanar distance and the overlap ratio) of dimer plays a vital role in the energy stability of the resultant excimer, together with the restricted relaxation of excited-state geometry in a rigid environment. Under free relaxation conditions, the excited-state geometry can generally be optimized into a completely parallel π–π stacking between two π–monomers, corresponding to the most stable excimer geometry in energy. Once deviated from this perfect excimer geometry, the emission properties of excimer will significantly change. In crystal **2**, the rigid xanthene frame restricts the free relaxation of two AN units, preventing intra-excimer formation in a perfectly parallel π–π stacking mode. As a consequence, this non-fully relaxed excited-state geometry leads to the formation of a metastable AN excimer and a blue-shift of its emission. On the contrary, due to the lack of a rigid frame template, the two AN units within the intermolecular π–π dimer, such as the dimers in crystal **1**, are able to undergo structural relaxation with almost complete freedom, achieving a more stable inter-excimer and a more redshifted emission.

To distinguish the differences in motion freedom of the AN units for inter-excimer and intra-excimer, temperature-dependent PL spectra were recorded for crystals **1** and **2**, respectively (Fig. 2c). With increasing temperature from 80 to 380 K, the PL spectrum of crystal **1** exhibited a gradual blueshift, while the PL peak of crystal **2** remained almost unchanged. Such an obvious difference can be ascribed to the more sensitive freedom of motion between two AN units in inter-excimer as compared to that in intra-excimer with increasing temperature. Due to the small motion constraint, the intermolecular π–π stacking in crystal **1** is susceptible to thermal fluctuations, leading to an increase in the average π–π distance of the inter-excimer geometry, as well as a consequent blueshift in the PL spectrum.[93] As a comparison, there was little effect on intramolecular π–π stacking (*e.g.*, π–π distance) in crystal **2** by temperature due to the restriction of the rigid xanthene frame in the crystal, resulting in insensitive temperature-dependence in the PL emission of intra-excimer. In addition, the dissimilar

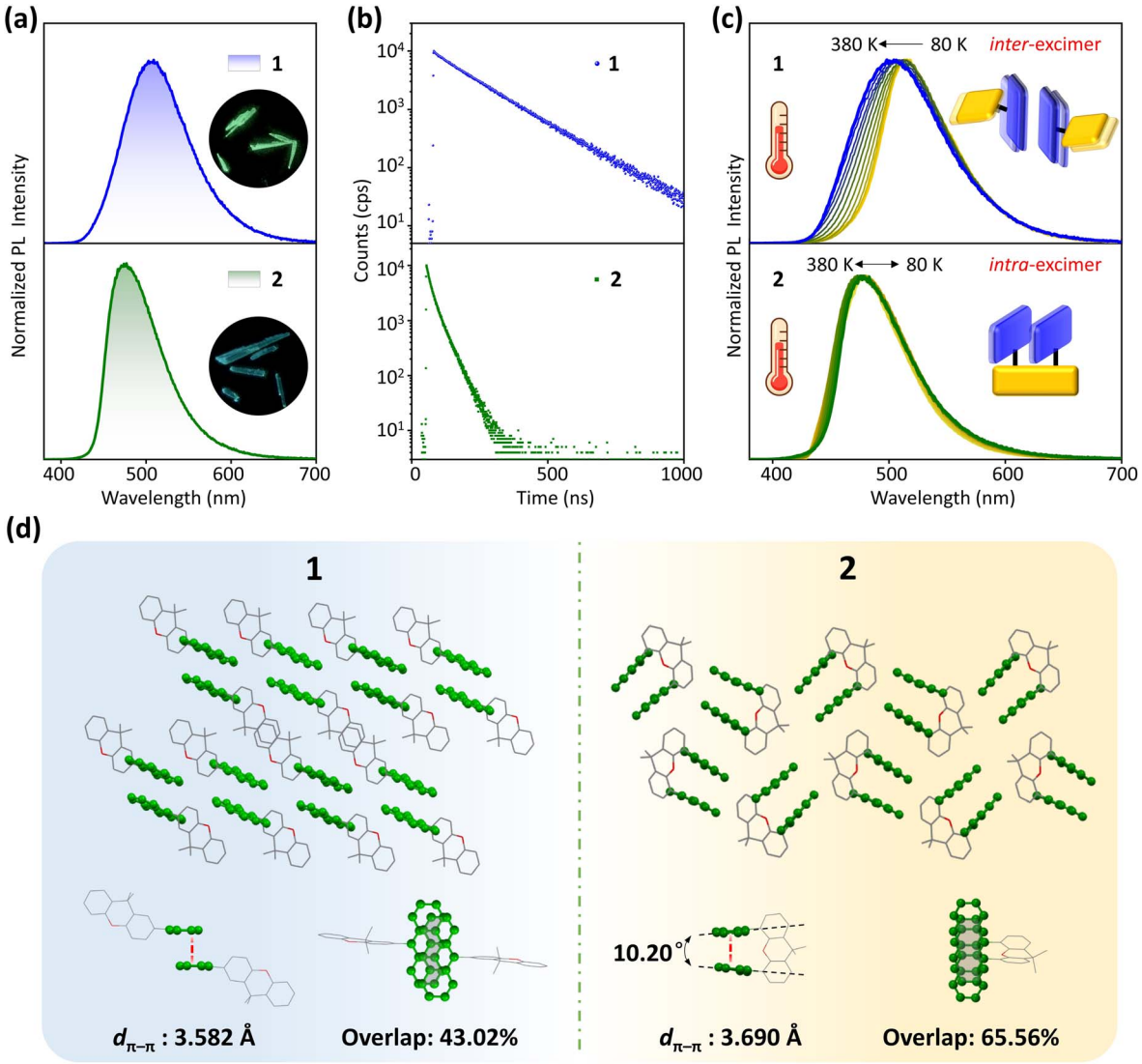

Fig. 2 (a) PL spectra and (b) time-resolved PL spectra of crystals **1** and **2**. (c) Temperature-dependent PL spectra of crystals **1** and **2**. (d) Molecular packing structures of crystals **1** and **2**.

fluorescence and molecular geometry between crystals **1** and **2** indicate that excimer formation is not only highly dependent on the mutual position and orientation between two AN units, but also closely related to the intermolecular interactions around them.

To describe the excited-state properties of excimers, time-dependent density functional theory (TD-DFT) calculations were performed for the pre-associated AN dimers within crystals **1** and **2**. Compared to their ground-state geometries, the $d_{\pi-\pi}$s values between ANs in the S_1 excited state are obviously decreased, indicative of 'compressed' geometry of the excited state (Fig. 3). The $d_{\pi-\pi}$ of optimized excited dimer **1** is 3.117 Å with a completely parallel cofacial π–π stacking, representing the most stable excimer geometry. Due to the restriction imposed by the xanthene frame, the AN planes in the **2** crystals cannot relax to the most stable equilibrium geometry. Consequently, the average $d_{\pi-\pi}$ is 3.241 Å, and the π–π planes deviate from parallel alignment, corresponding to a metastable AN excimer state. The natural transition orbitals (NTOs) for the S_1 state of dimer in crystal **1** exhibit a hybridized local and charge-transfer (HLCT) character, indicating typical intermolecular AN excimer emission in the **1** crystals.[94] The HLCT state also occurred on two π–π stacking AN units for the S_1 state of dimer in crystal **2**, which indicates that an intra-excimer formed between two AN units upon excitation. Furthermore, we evaluated the charge-transfer (CT) content of two dimers in the S_1 state (Fig. S9–S11 and Table S4†).[95] The CT content in dimer **1** is higher than that in dimer **2**, corresponding to a redshifted emission wavelength in the former.

Interestingly, crystal **1** with an extended lifetime exhibits the highest PLQY, up to 83.96%, while crystal **2** demonstrates a PLQY of 42.27%. It can be clearly shown there is a higher PLQY for the static excimer in the intermolecular state as compared to the corresponding monomer, which is completely

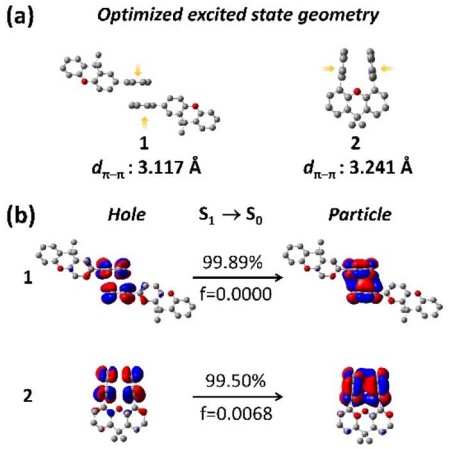

Fig. 3 (a) Optimized excited state geometries and (b) NTOs of excimers **1** and **2**.

different from the commonly believed low PLQY of excimer fluorescence. According to the PLQY and lifetime values (Fig. 4a), the inter-excimer in crystal **1** exhibits a more significant reduction in k_{nr} (1.05×10^6 s^{-1}) as compared to that of crystal **2** (1.43×10^7 s^{-1}), which is ascribed to the more rigid inter-excimer geometry for more effective non-radiation suppression in the former, as a result of the closer π–π distance in the equilibrium geometry by intermolecular CT interactions from the HLCT state. For the purpose of comparison, compound **2** was dispersed into a polymer matrix of 1 wt% polymethyl methacrylate (PMMA) to form the single-molecule doped film (Fig. S12†). The PL spectrum of **2** in the solid film exhibits $\lambda_{max} = 482$ nm. Such a good PL consistency suggests the formation of very similar intra-excimer in the doped film and crystal **2**. Importantly, due to preventing intermolecular interactions between adjacent AN dimers, the PLQY of the **2**-doped film (77.12%) was obviously improved relative to that of crystal **2**, but still lower than that of crystal **1** (83.96%). This result confirms yet again that the discrete dimer of π–π stacking is surely beneficial to excimer formation with high-efficiency fluorescence. Importantly, the greater the stability of the formed excimer, the higher its fluorescence PLQY. It is easier to achieve a higher PLQY with the inter-excimer as compared with the intra-excimer under static conditions because of the higher energy stability and the more effective non-radiative suppression of the inter-excimer excited state (Fig. 4b). As for the static environment, these observations suggest that intermolecular interactions within the crystals play a crucial role in the PLQY of excimer fluorescence, and they are not only responsible for the excimer formation probability, but they also contribute to the suppression of non-radiation.

Comparison between inter-excimer and intra-excimer

In crystals **1** and **2**, the stronger π–π interactions between two AN units facilitated excimer formation in rigid environments, leading to higher PLQY of excimer fluorescence compared to dynamic excimer formed in solutions. Due to the discrete π–π stacking of AN dimers, stable inter-excimer formation and greatly localized excitons further facilitated the highest PLQY of excimer fluorescence in crystal **1**. In contrast, metastable intra-excimer was formed with moderate PLQY of excimer emission in crystal **2** as a result of the restricted geometric relaxation caused by the rigid frame template (Fig. 4b).

Conclusively, based on the above observations, the excimer fluorescence efficiency can be ranked from low to high: dynamic inter-excimer < dynamic intra-excimer < static intra-excimer < static inter-excimer (Fig. 5a). This ranking highlights the important roles of environmental rigidity and energy stability of excited states in the PLQY of excimer fluorescence. These results suggest that in a rigid environment, the most stable excimer formation between two AN units can facilitate the achievement of highly efficient excimer fluorescence. Further systematic investigation of this idea is necessary for general validation and widespread support.

In this work, some rules can be summarized by a careful comparison between inter-excimer and intra-excimer (Fig. 5b). First, in a dynamic environment, the intra-excimer can effectively form and maintain the dominant excimer fluorescence even in a dilute solution, while the inter-excimer is produced only in a concentrated solution exhibiting major monomer and minor excimer emissions. Second, in a static environment, the

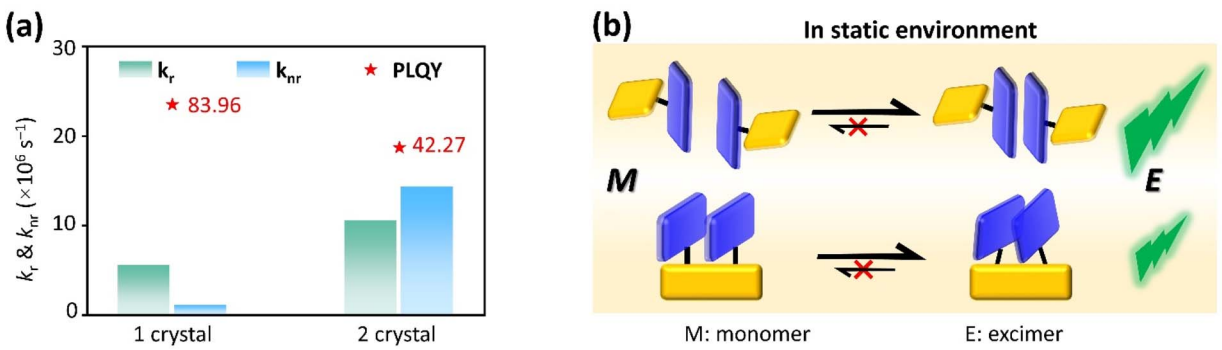

Fig. 4 (a) PLQYs, k_rs and k_{nr}s of crystals **1** and **2**. (b) Schematic diagram of inter-excimer and intra-excimer in a static environment. In a static environment, due to the restriction of the intramolecular template, intra-excimer could only assume a metastable state, while inter-excimer could readily relax to the most stable equilibrium geometry.

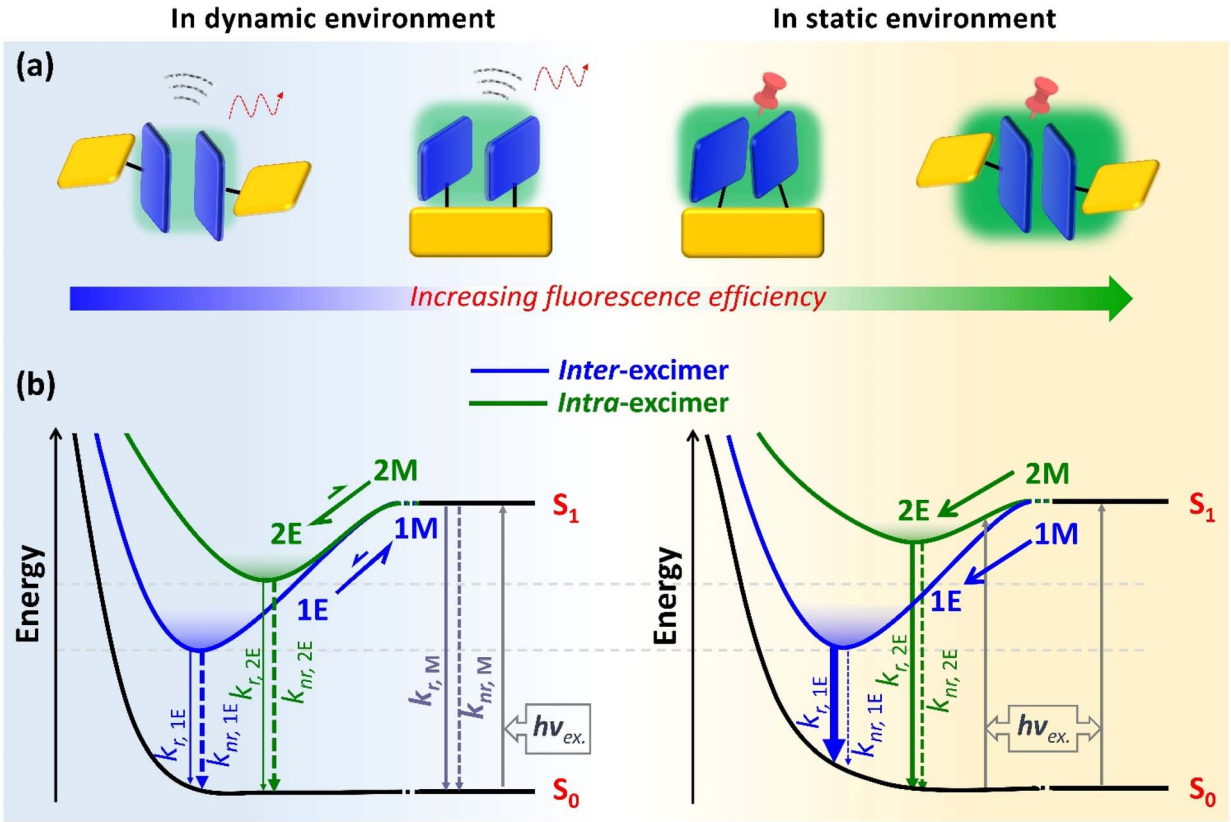

Fig. 5 (a) Diagram of the relationship between excimer species and PLQY. (b) Schematic diagrams of the fluorescent mechanism of excimers in dynamic and static environments. M denotes monomer, and E denotes excimer.

inter-excimer can readily undergo structural relaxation to achieve the most stable equilibrium geometry, while the intra-excimer can only form a metastable state due to the limitations and constraints of the rigid frame template. Third, in terms of synthetic complexity, there is a greater degree of difficulty in the synthesis of intra-excimer as compared to the non-covalent monomer-based assembly of inter-excimer. Finally, in terms of processability, it is easier to prepare thin films of intra-excimer by either evaporation or solution processing as compared to the inter-excimer, which is problematic in amorphous film preparation, especially for inter-excimer formation in a rigid environment. This work provides a systematic investigation and careful comparison of excited-state formation and photophysical properties between intra-excimer and inter-excimer. A comprehensive understanding of excimer is very important for fundamental implications and practical applications in the development of high-performance fluorescent materials.

Conclusions

An AN-based inter-excimer and intra-excimer were constructed using a rigid xanthene frame template as a spacer and a linker, respectively. Their photophysical properties were systematically investigated in dynamic (solution) and static (crystal) environments. In the solution state, both inter-excimer and intra-excimer formation led to fluorescence quenching relative to the monomer emission, which is generally considered to be a poor-emissive defect or energy trap. This situation was attributed to the limited formation and ease of dissociation of the excimer in a dynamic environment, together with the dominant non-radiative transition and the forbidden radiation nature of the excimer state. Furthermore, the intra-excimer exhibited an increased PLQY compared to the inter-excimer, arising from the rigid frame template that improved the formation and restricted the disassociation of the intra-excimer. As a comparison, the inter-excimer and intra-excimer in the crystal display significantly enhanced PLQYs relative to those in a dynamic environment. This PLQY enhancement can be ascribed to the substantially suppressed non-radiation by the excimer itself and the static environment (the efficient formation and non-dissociation of the excimer), despite the forbidden radiative transition nature of the excimer. Additionally, because the AN dimer forms a more stable inter-excimer in a discrete π–π stacking mode, the inter-excimer exhibits a higher PLQY than the intra-excimer, with restricted relaxation caused by the rigid frame template in the crystal. We performed a systematical investigation and careful comparison between the inter-excimer and intra-excimer, which not only provides a comprehensive understanding of excimer formation and photophysical properties, but also suggests a new design strategy for non-covalent dimers for high-performance fluorescent materials.

Data availability

All necessary information is included in the ESI.†

Author contributions

Conceptualization: H. Liu, S.-T. Zhang, and B. Yang. Data curation: S. Wang, S. Zhao, Z. Yang, D. Yang, and Y. Lv. Chemical synthesis and product analysis: S. Wang, D. Yang, Q. Wu, and Q. Su. DFT calculations: S. Wang, H. Liu, and Z. Yang. Supervision: H. Liu and B. Yang. Funding acquisition: H. Liu and B. Yang. Writing original draft: S. Wang. Writing – review and editing: H. Liu and B. Yang.

Conflicts of interest

There are no conflicts to declare.

Acknowledgements

We thank Z. Guo of Tianjin University for assistance with useful discussions. This work is supported by the National Natural Science Foundation of China (52073117, 52103209, and 52373183), the National Key Research and Development Program of China (No. 2020YFA0714603), and the Open Project of the State Key Laboratory of Supramolecular Structure and Materials (sklssm2024026).

References

1 T. M. Figueira-Duarte and K. Müllen, *Chem. Rev.*, 2011, **111**, 7260–7314.
2 Y. Wang, J. Nie, W. Fang, L. Yang, Q. Hu, Z. Wang, J. Z. Sun and B. Z. Tang, *Chem. Rev.*, 2020, **120**, 4534–4577.
3 H. Jiang, S. Zhu, Z. Cui, Z. Li, Y. Liang, J. Zhu, P. Hu, H.-L. Zhang and W. Hu, *Chem. Soc. Rev.*, 2022, **51**, 3071–3122.
4 L. Tu, Y. Xie, Z. Li and B. Tang, *SmartMat*, 2021, **2**, 326–346.
5 Q. Li and Z. Li, *Acc. Chem. Res.*, 2020, **53**, 962–973.
6 Q. Li and Z. Li, *Adv. Sci.*, 2017, **4**, 1600484.
7 F. Würthner, *Angew. Chem., Int. Ed.*, 2020, **59**, 14192–14196.
8 L. Catti, H. Narita, Y. Tanaka, H. Sakai, T. Hasobe, N. V. Tkachenko and M. Yoshizawa, *J. Am. Chem. Soc.*, 2021, **143**, 9361–9367.
9 Y.-H. Chen, K.-C. Tang, Y.-T. Chen, J.-Y. Shen, Y.-S. Wu, S.-H. Liu, C.-S. Lee, C.-H. Chen, T.-Y. Lai, S.-H. Tung, R.-J. Jeng, W.-Y. Hung, M. Jiao, C.-C. Wu and P.-T. Chou, *Chem. Sci.*, 2016, **7**, 3556–3563.
10 H. Qi, C. Zhang, Z. Huang, L. Wang, W. Wang and A. J. Bard, *J. Am. Chem. Soc.*, 2016, **138**, 1947–1954.
11 H. L. Lee, S. O. Jeon, I. Kim, S. C. Kim, J. Lim, J. Kim, S. Park, J. Chwae, W.-J. Son, H. Choi and J. Y. Lee, *Adv. Mater.*, 2022, **34**, 2202464.
12 H.-H. Cho, D. G. Congrave, A. J. Gillett, S. Montanaro, H. E. Francis, V. Riesgo-Gonzalez, J. Ye, R. Chowdury, W. Zeng, M. K. Etherington, J. Royakkers, O. Millington, A. D. Bond, F. Plasser, J. M. Frost, C. P. Grey, A. Rao, R. H. Friend, N. C. Greenham and H. Bronstein, *Nat. Mater.*, 2024, **23**, 519–526.
13 X. He, J. Lou, B. Li, X. Dong, F. Zhong, W. Liu, X. Feng, D. Yang, D. Ma, Z. Zhao, Z. Wang and B. Z. Tang, *Adv. Mater.*, 2024, **36**, 2310417.
14 R. Guo, W. Liu, S. Ying, Y. Xu, Y. Wen, Y. Wang, D. Hu, X. Qiao, B. Yang, D. Ma and L. Wang, *Sci. Bull.*, 2021, **66**, 2090–2098.
15 Z. Zhang, Y. Zhang, D. Yao, H. Bi, I. Javed, Y. Fan, H. Zhang and Y. Wang, *Cryst. Growth Des.*, 2009, **9**, 5069–5076.
16 J. Mei, N. L. C. Leung, R. T. K. Kwok, J. W. Y. Lam and B. Z. Tang, *Chem. Rev.*, 2015, **115**, 11718–11940.
17 Y. Hong, J. W. Y. Lam and B. Z. Tang, *Chem. Soc. Rev.*, 2011, **40**, 5361–5388.
18 Y. Hong, J. W. Y. Lam and B. Z. Tang, *Chem. Commun.*, 2009, 4332–4353, DOI: **10.1039/B904665H**.
19 T. Förster, *Angew Chem. Int. Ed. Engl.*, 1969, **8**, 333–343.
20 J. B. Birks, *Rep. Prog. Phys.*, 1975, **38**, 903.
21 B. Stevens and E. Hutton, *Nature*, 1960, **186**, 1045–1046.
22 J. B. Birks and L. G. Christophorou, *Spectrochim. Acta*, 1963, **19**, 401–410.
23 F. M. Winnik, *Chem. Rev.*, 1993, **93**, 587–614.
24 J. Hoche, H.-C. Schmitt, A. Humeniuk, I. Fischer, R. Mitrić and M. I. S. Röhr, *Phys. Chem. Chem. Phys.*, 2017, **19**, 25002–25015.
25 T. Förster and K. Kasper, *Zeitschrift für Elektrochemie, Berichte der Bunsengesellschaft für physikalische Chemie*, 1955, **59**, 976–980.
26 J. B. Aladekomo, J. B. Birks and B. H. Flowers, *Proc. R. Soc. London, Ser. A*, 1965, **284**, 551–565.
27 A. Yadav, N. D. Kurur and S. Pandey, *J. Phys. Chem. B*, 2015, **119**, 13367–13378.
28 R. V. Todesco and J. Put, *J. Photochem.*, 1986, **34**, 305–322.
29 K. A. Zachariasse, W. Kuehnle, U. Leinhos, P. Reynders and G. Striker, *J. Phys. Chem.*, 1991, **95**, 5476–5488.
30 R. Todesco, J. Gelan, H. Martens, J. Put and F. C. De Schryver, *J. Am. Chem. Soc.*, 1981, **103**, 7304–7312.
31 Z.-H. Tong, Y.-Y. Liu and C.-B. Xu, *Acta Chim. Sin.*, 1988, **6**, 52–61.
32 K. E. Brown, W. A. Salamant, L. E. Shoer, R. M. Young and M. R. Wasielewski, *J. Phys. Chem. Lett.*, 2014, **5**, 2588–2593.
33 V. A. Spata and S. Matsika, *J. Phys. Chem. A*, 2013, **117**, 8718–8728.
34 I. Conti, A. Nenov, S. Höfinger, S. Flavio Altavilla, I. Rivalta, E. Dumont, G. Orlandi and M. Garavelli, *Phys. Chem. Chem. Phys.*, 2015, **17**, 7291–7302.
35 M. Dvořák, S. K. K. Prasad, C. B. Dover, C. R. Forest, A. Kaleem, R. W. MacQueen, A. J. Petty II, R. Forecast, J. E. Beves, J. E. Anthony, M. J. Y. Tayebjee, A. Widmer-Cooper, P. Thordarson and T. W. Schmidt, *J. Am. Chem. Soc.*, 2021, **143**, 13749–13758.
36 N. Dey and S. Bhattacharya, *Anal. Chem.*, 2017, **89**, 10376–10383.
37 F. C. De Schryver, P. Collart, J. Vandendriessche, R. Goedeweeck, A. M. Swinnen and M. Van der Auweraer, *Acc. Chem. Res.*, 1987, **20**, 159–166.

38 T. Kindt, E.-P. Resewitz, C. Goedicke and E. Lippert, *Z. Phys. Chem.*, 1976, **101**, 1–10.
39 K. A. Zachariasse, G. Duveneck and W. Kühnle, *Chem. Phys. Lett.*, 1985, **113**, 337–343.
40 E. A. Margulies, L. E. Shoer, S. W. Eaton and M. R. Wasielewski, *Phys. Chem. Chem. Phys.*, 2014, **16**, 23735–23742.
41 H. Yoo, J. Yang, A. Yousef, M. R. Wasielewski and D. Kim, *J. Am. Chem. Soc.*, 2010, **132**, 3939–3944.
42 R. J. Lindquist, K. M. Lefler, K. E. Brown, S. M. Dyar, E. A. Margulies, R. M. Young and M. R. Wasielewski, *J. Am. Chem. Soc.*, 2014, **136**, 14912–14923.
43 R. E. Cook, B. T. Phelan, R. J. Kamire, M. B. Majewski, R. M. Young and M. R. Wasielewski, *J. Phys. Chem. A*, 2017, **121**, 1607–1615.
44 Y. J. Bae, D. Shimizu, J. D. Schultz, G. Kang, J. Zhou, G. C. Schatz, A. Osuka and M. R. Wasielewski, *J. Phys. Chem. A*, 2020, **124**, 8478–8487.
45 J. Wang, Q. Dang, Y. Gong, Q. Liao, G. Song, Q. Li and Z. Li, *CCS Chem.*, 2021, **3**, 274–286.
46 Q. Liao, A. Li, A. Huang, J. Wang, K. Chang, H. Li, P. Yao, C. Zhong, P. Xie, J. Wang, Z. Li and Q. Li, *Chem. Sci.*, 2024, **15**, 4364–4373.
47 J. Suk, Z. Wu, L. Wang and A. J. Bard, *J. Am. Chem. Soc.*, 2011, **133**, 14675–14685.
48 H. Osaki, C.-M. Chou, M. Taki, K. Welke, D. Yokogawa, S. Irle, Y. Sato, T. Higashiyama, S. Saito, A. Fukazawa and S. Yamaguchi, *Angew. Chem., Int. Ed.*, 2016, **55**, 7131–7135.
49 J. Sung, A. Nowak-Król, F. Schlosser, B. Fimmel, W. Kim, D. Kim and F. Würthner, *J. Am. Chem. Soc.*, 2016, **138**, 9029–9032.
50 J.-Y. Hu, Y.-J. Pu, G. Nakata, S. Kawata, H. Sasabe and J. Kido, *Chem. Commun.*, 2012, **48**, 8434–8436.
51 C. M. Mauck, R. M. Young and M. R. Wasielewski, *J. Phys. Chem. A*, 2017, **121**, 784–792.
52 H. Zhang, J. Han, X. Jin and P. Duan, *Angew. Chem., Int. Ed.*, 2021, **60**, 4575–4580.
53 C. Shang, G. Wang, Y.-C. Wei, Q. Jiang, K. Liu, M. Zhang, Y.-Y. Chen, X. Chang, F. Liu, S. Yin, P.-T. Chou and Y. Fang, *CCS Chem.*, 2022, **4**, 1949–1960.
54 N. J. Hestand and F. C. Spano, *Chem. Rev.*, 2018, **118**, 7069–7163.
55 M. Yoshizawa and L. Catti, *Acc. Chem. Res.*, 2019, **52**, 2392–2404.
56 G. Wu, F. Li, B. Tang and X. Zhang, *J. Am. Chem. Soc.*, 2022, **144**, 14962–14975.
57 L. S. Kaanumalle, C. L. D. Gibb, B. C. Gibb and V. Ramamurthy, *J. Am. Chem. Soc.*, 2005, **127**, 3674–3675.
58 G. Wu, I. Szabó, E. Rosta and O. A. Scherman, *Chem. Commun.*, 2019, **55**, 13227–13230.
59 G. Wu, Y. J. Bae, M. Olesińska, D. Antón-García, I. Szabó, E. Rosta, M. R. Wasielewski and O. A. Scherman, *Chem. Sci.*, 2020, **11**, 812–825.
60 J. Wang, Z. Huang, X. Ma and H. Tian, *Angew. Chem., Int. Ed.*, 2020, **59**, 9928–9933.
61 H. Wu, Y. Wang, L. O. Jones, W. Liu, B. Song, Y. Cui, K. Cai, L. Zhang, D. Shen, X.-Y. Chen, Y. Jiao, C. L. Stern, X. Li, G. C. Schatz and J. F. Stoddart, *J. Am. Chem. Soc.*, 2020, **142**, 16849–16860.
62 B. Tang, W.-L. Li, Y. Chang, B. Yuan, Y. Wu, M.-T. Zhang, J.-F. Xu, J. Li and X. Zhang, *Angew. Chem., Int. Ed.*, 2019, **58**, 15526–15531.
63 K. Kudo, T. Ide, N. Kishida and M. Yoshizawa, *Angew. Chem., Int. Ed.*, 2021, **60**, 10552–10556.
64 D. Guo, W. Wang, K. Zhang, J. Chen, Y. Wang, T. Wang, W. Hou, Z. Zhang, H. Huang, Z. Chi and Z. Yang, *Nat. Commun.*, 2024, **15**, 3598.
65 C. Lv, W. Liu, Q. Luo, H. Yi, H. Yu, Z. Yang, B. Zou and Y. Zhang, *Chem. Sci.*, 2020, **11**, 4007–4015.
66 J. Ochi, K. Tanaka and Y. Chujo, *Angew. Chem., Int. Ed.*, 2023, **62**, e202214397.
67 Y. Ai, M. H.-Y. Chan, A. K.-W. Chan, M. Ng, Y. Li and V. W.-W. Yam, *Proc. Natl. Acad. Sci. U. S. A.*, 2019, **116**, 13856–13861.
68 Y. Zhang, H. Yang, H. Ma, G. Bian, Q. Zang, J. Sun, C. Zhang, Z. An and W.-Y. Wong, *Angew. Chem., Int. Ed.*, 2019, **58**, 8773–8778.
69 X. Shan, W. Chi, H. Jiang, Z. Luo, C. Qian, H. Wu and Y. Zhao, *Angew. Chem., Int. Ed.*, 2023, **62**, e202215652.
70 J. Ochi, K. Tanaka and Y. Chujo, *Angew. Chem., Int. Ed.*, 2020, **59**, 9841–9855.
71 K. Wada, K. Hashimoto, J. Ochi, K. Tanaka and Y. Chujo, *Aggregate*, 2021, **2**, e93.
72 K. Yuhara and K. Tanaka, *Angew. Chem., Int. Ed.*, 2024, **63**, e202319712.
73 M. Mahl, K. Shoyama, A.-M. Krause, D. Schmidt and F. Würthner, *Angew. Chem., Int. Ed.*, 2020, **59**, 13401–13405.
74 R. M. Young and M. R. Wasielewski, *Acc. Chem. Res.*, 2020, **53**, 1957–1968.
75 M.-C. Tang, Y.-C. Wei, Y.-C. Chu, C.-X. Jiang, Z.-X. Huang, C.-C. Wu, T.-H. Chao, P.-H. Hong, M.-J. Cheng, P.-T. Chou and Y.-T. Wu, *J. Am. Chem. Soc.*, 2020, **142**, 20351–20358.
76 D.-G. Chen, Y. Chen, C.-H. Wu, Y.-A. Chen, M.-C. Chen, J.-A. Lin, C.-Y. Huang, J. Su, H. Tian and P.-T. Chou, *Angew. Chem., Int. Ed.*, 2019, **58**, 13297–13301.
77 L. Wang, W.-Y. Wong, M.-F. Lin, W.-K. Wong, K.-W. Cheah, H.-L. Tam and C. H. Chen, *J. Mater. Chem.*, 2008, **18**, 4529–4536.
78 S. Hisamatsu, H. Masu, M. Takahashi, K. Kishikawa and S. Kohmoto, *Cryst. Growth Des.*, 2015, **15**, 2291–2302.
79 Y. Ge, Y. Wen, H. Liu, T. Lu, Y. Yu, X. Zhang, B. Li, S.-T. Zhang, W. Li and B. Yang, *J. Mater. Chem. C*, 2020, **8**, 11830–11838.
80 H. Liu, L. Yao, B. Li, X. Chen, Y. Gao, S. Zhang, W. Li, P. Lu, B. Yang and Y. Ma, *Chem. Commun.*, 2016, **52**, 7356–7359.
81 H. Liu, D. Cong, B. Li, L. Ye, Y. Ge, X. Tang, Y. Shen, Y. Wen, J. Wang, C. Zhou and B. Yang, *Cryst. Growth Des.*, 2017, **17**, 2945–2949.
82 Y. Shen, H. Liu, S. Zhang, Y. Gao, B. Li, Y. Yan, Y. Hu, L. Zhao and B. Yang, *J. Mater. Chem. C*, 2017, **5**, 10061–10067.
83 Y. Shen, Z. Zhang, H. Liu, Y. Yan, S. Zhang, B. Yang and Y. Ma, *J. Phys. Chem. C*, 2019, **123**, 13047–13056.
84 S. Sekiguchi, K. Kondo, Y. Sei, M. Akita and M. Yoshizawa, *Angew. Chem., Int. Ed.*, 2016, **55**, 6906–6910.

85 S. K. Mohan Nalluri, J. Zhou, T. Cheng, Z. Liu, M. T. Nguyen, T. Chen, H. A. Patel, M. D. Krzyaniak, W. A. Goddard III, M. R. Wasielewski and J. F. Stoddart, *J. Am. Chem. Soc.*, 2019, **141**, 1290–1303.
86 M. M. Safont-Sempere, P. Osswald, K. Radacki and F. Würthner, *Chem.–Eur. J.*, 2010, **16**, 7380–7384.
87 Y. Wang, H. Wu and J. F. Stoddart, *Acc. Chem. Res.*, 2021, **54**, 2027–2039.
88 H. Liu, Y. Shen, Y. Yan, C. Zhou, S. Zhang, B. Li, L. Ye and B. Yang, *Adv. Funct. Mater.*, 2019, **29**, 1901895.
89 Y. Dai, H. Liu, T. Geng, F. Ke, S. Niu, K. Wang, Y. Qi, B. Zou, B. Yang, W. L. Mao and Y. Lin, *J. Mater. Chem. C*, 2021, **9**, 934–938.
90 H. Liu, Y. Gu, Y. Dai, K. Wang, S. Zhang, G. Chen, B. Zou and B. Yang, *J. Am. Chem. Soc.*, 2020, **142**, 1153–1158.
91 P. E. Fielding and R. C. Jarnagin, *J. Chem. Phys.*, 1967, **47**, 247–252.
92 H. D. Becker, K. Sandros, B. W. Skelton and A. H. White, *J. Phys. Chem.*, 1981, **85**, 2930–2933.
93 Y. Shen, H. Liu, J. Cao, S. Zhang, W. Li and B. Yang, *Phys. Chem. Chem. Phys.*, 2019, **21**, 14511–14515.
94 Y. Gao, H. Liu, S. Zhang, Q. Gu, Y. Shen, Y. Ge and B. Yang, *Phys. Chem. Chem. Phys.*, 2018, **20**, 12129–12137.
95 T. Lu and F. Chen, *J. Comput. Chem.*, 2012, **33**, 580–592.